15th Triennial World Congress, Barcelona, Spain

STABILISATION OF A 12 DEGREE OF FREEDOM BIPED ROBOT

G. A. Medrano-Cerda and D. Akdas

School of Acoustics and Electronic Engineering, University of Salford
Salford M5 4WT, UK
g.a.medrano-cerda@eee.salford.ac.uk
Department of Mechanical Engineering, Balikesir University, Balikesir, Tutkey
davut_akdas@hotmail.com

Abstract: This paper considers the design and evaluation of stabilising controllers for a twelve degree of freedom biped robot using linear quadratic optimal control techniques and reduced order observers. The controllers are designed using approximate planar dynamical models for the sagittal and lateral planes. Experiments were carried out to test the control system when the biped robot was in the double support phase and during locomotion. Although the control system is based on single support models, the experimental results have shown that the robot successfully kept its given posture.

Keywords: Biped Robot, Optimal Control, Stabilisation

1. INTRODUCTION

In recent years, there has been an increased interest in bipedal robots. In particular, the creation of a European Network on Climbing and Walking Robots (CLAWAR) has provided a focus for worldwide research on mobile robotics. Experimental prototypes have been developed throughout the world and at present, the most remarkable results have been achieved by (Hirai, et al., 1998). Several researchers have investigated stabilisation strategies based on modern control theory and linearized (planar) models. (Mita, et al., 1984) used linear optimal regulator theory; (Eldukhri, 1996) and (Medrano-Cerda and Eldukhri, 1997) considered linear optimal control implemented via reduced order observers. (Hemami and Wyman, 1979) and (Golliday and Hemami, 1976) used pole placement controllers in their simulation studies; decoupling control was studied by (Raibert, 1986) and (Golliday and Hemami, 1977. (Miura and Shimoyama, 1984) used linear state feedback to stabilise motions around carefully pre-selected trajectories. (Channon, et al., 1992) used local PD joint controllers with gravity compensation and gain scheduling; slow motion stabilisation was achieved by controlling the position of the centre of gravity. (Inaba, et al., 1995) followed a similar approach for static balancing using vision feedback to control the position of the centre of gravity. For high speed locomotion, the problem of maintaining balance involves controlling the position of the zero moment point (ZMP) (Vukobratovic, et al., 1990). For a biped with a trunk the ZMP method is outlined in (Takanishi, et al., 1985, 1990). Refinements and variations to the basic ZMP approach are considered in (Li, et al., 1993), (Yamaguchi, et al., 1999). The humanoid robot developed by (Hirai, et al., 1998) is also based on the ZMP method. The authors claim that their stabilising controller is similar to that of humans, yet when walking or standing on flat surfaces the angles in the sagittal plane are rather large. This is particularly noticeable in the knee joints. Experimental results in (Eldukhri, 1996) and (Medrano-Cerda and Eldukhri, 1997) showed that during the single support phase the leg joints could be straightened and while standing on both feet small angles could be maintained to reduce power consumption. The experimental tests were carried out using a prototype with eight degrees of freedom, seven in the sagittal plane and one in the lateral plane (trunk). This joint distribution limited the robot locomotion to the sagittal plane. Four additional degrees of freedom were needed for locomotion in the lateral plane (ankles and hips).

The work in this paper is an extension of our previous research to include multiple degrees of freedom in both sagittal and lateral planes. To simplify the design, independent stabilising controllers are developed for the sagittal and lateral planes. A brief description of the new biped robot is

given in section 2. The techniques used for derivation of mathematical models and the designs of the control systems are presented in section 3. Robustness and disturbance transmission properties of the control systems are assessed in section 4. Conclusions are given in section 5.

2. SYSTEM DESCRIPTION

The biped robot has twelve degrees of freedom, five in the lateral plane and seven in the sagittal plane: 2DOF ankle, 2DOF hip, 2DOF trunk and 1DOF knee joints. Figure 2.1 shows joints distribution. The joints are driven by permanent magnet DC motors and low backlash gearboxes. Potentiometers measure relative joint angles. Force sensors underneath each foot are used to measure ground reaction forces in the sagittal and lateral planes. The robot weights 17.8kg and is 1.75m tall. The foot size is 0.18m wide by 0.3m long. The biped is controlled by 486DX20 PC. Smoothing and anti-aliasing filters (at 15 Hz and 22 Hz respectively) are used for signal conditioning.

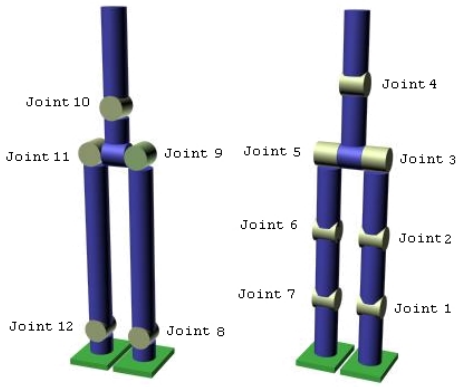

Fig. 2.1 Lateral and sagittal joints of the biped robot

3. MODELLING AND CONTROL SYSTEM DESIGN

Symbolic mathematical models of the biped are obtained for the sagittal and lateral planes separately. This reduces the complexity of the symbolic model. It is assumed that the robot is in the single support phase (open chain structure), the support foot is in firm contact with the ground and that slippage does not occur. The ankle joint of the swing leg has a small contribution to the dynamic equations. Therefore this joint is neglected in the derivation of mathematical model. However, the mass of the swing-leg foot is added to the mass of the corresponding knee link. Joint viscous friction and motor inductance are neglected. Stiction and backlash in the gearboxes are not included in the models. Different modelling formulations are available: Lagrangian dynamics (Lewis, et al., 1993), Newton-Euler equations (Vukobratovic, et al., 1990) and Kane's equations of motion (Amirouche 1992). The reduced model for the sagittal plane has six links: lower and upper support leg, hip, trunk, upper swing leg and lower swing leg+foot. To keep the swing-leg foot parallel to the ground a separate foot controller is used. The non-linear model takes the form

$$J_s(\theta)\ddot{\theta} + X_s(\theta)\dot{\theta}^2 + Y_s\dot{\theta} + Z_s(\theta) = f_s \qquad (1)$$

Here θ, $\dot{\theta}$ and $\ddot{\theta}$ denote absolute joint angles, angular velocities and accelerations, respectively. Motor voltages and disturbance torques are included in f_s. Linearizing around the upright position and using a 10ms sampling time interval, we obtain a linear discrete time model in state space form

$$x_s(k+1) = A_s x_s(k) + B_s u_s(k) + B_s^{dist}\tau_s(k) \qquad (2)$$
$$x_{s1}(k) = C_s x_s(k) \qquad (3)$$
$$x_s = \begin{bmatrix} x_{s1}{}^T & x_{s2}{}^T \end{bmatrix}^T$$

Here A_s, B_s, B_s^{dist} and C_s are the state space matrices in the sagittal plane. The control signal is denoted by u_s, x_{s1} represents relative angular displacements, x_{s2} relative angular velocities and τ_s denotes disturbance torques. The mathematical model for the lateral plane is derived in the same way as for the sagittal plane, but only with four links: support leg, hip, trunk and swing leg+foot. The non-linear model is linearized about the vertical except the hip link, which is linearized about the horizontal. The equations for the lateral plane are similar to (1)-(3).

3.1 Observer design.

To estimate relative angular velocities a reduced order observer is designed for each plane. Both models are observable and this ensures that state observers with arbitrarily chosen dynamics can be designed. The structure of the observer is given below for the sagittal plane

$$z_s(k) = F_s z_s(k) + E_s x_{s1}(k) + H_s u_s(k)$$
$$\hat{x}_{s2}(k) = z_s(k) + K_s x_{s1}(k) \qquad (4)$$

The torque disturbances are excluded in the observer since they are not measured or known accurately. Once the observer dynamics F_s are chosen, the remaining observer parameters are computed from the following relations

$$A_s = \begin{bmatrix} A_{s11} & A_{s12} \\ A_{s21} & A_{s22} \end{bmatrix},\ B_s = \begin{bmatrix} B_{s1} \\ B_{s2} \end{bmatrix}$$
$$K_s = (A_{s22} - F_s)A_{s12}{}^{-1}$$
$$H_s = B_{s2} - K_s B_{s1}$$
$$E_s = (A_{s21} - K_s A_{s11}) + F_s K_s$$

Selecting $F_s = 0.9I_{6\times6}$ ($I_{6\times6} = 6\times6$ identity matrix) reduces estimation errors quickly without degrading stability margins too much. The observer for the lateral plane has the same structure as the one given above but $F_l = 0.9I_{4\times4}$.

3.2 Control system design.

The stabilising control systems incorporate state feedback (reduced order observers estimate the relative angular velocities), integral action to reduce the steady state errors and a feedforward term to speed up tracking of reference signals. The controller structure for the sagittal plane is

$$u_s(k) = -L2_s\, x_{as}(k) - L11_s\, x_{s1}(k) - L12_s\, \hat{x}_{s2}(k) + Lff_s\, r_s(k) \quad (5)$$

where $L11_s$ is the gain associated with the relative angles, $L12_s$ is for the relative angular velocities and $L2_s$ is for the integral actions. The feed forward gain Lff_s is set equal to $L11_s$. The feed forward term is particularly useful when small integral gains are used. If the integrators have large gains it is better to set L_{ffs} equal to zero. The state space equation of the integral action is

$$x_{as}(k+1) = x_{as}(k) + u_{as}(k) \quad (6)$$
$$u_{as}(k) = r_s(k) - x_{s1}(k)$$

Here x_{as} is the state vector for the integrators and r_s is the reference signal, which is set to zero in the Linear Quadratic Regulator design. The design of the optimal state feedback matrix starts with the specification of a quadratic performance index

$$J_s = \sum_{k=0}^{\infty} \left(x_{ds}(k)^T Q_{ds} x_{ds}(k) + u_s(k)^T R_{ds} u_s(k) \right) \quad (7)$$

Where Q_{ds} and R_{ds} are chosen as diagonal matrices with positive entries. The constraint equation is (ignoring torque disturbances)

$$x_{ds}(k+1) = \Phi_{ds}\, x_{ds}(k) + \Gamma_{ds}\, u_s(k) \quad (8)$$

Where $x_{ds} = \begin{bmatrix} x_s \\ x_{as} \end{bmatrix}$, $\Phi_{ds} = \begin{bmatrix} A_s & 0_{12\times 6} \\ -C_s & I_{6\times 6} \end{bmatrix}$ and $\Gamma_{ds} = \begin{bmatrix} B_s \\ 0_{6\times 6} \end{bmatrix}$

The selection of Q_{ds} and R_{ds} was investigated in Matlab simulations and during experiments. The aims were to achieve fast response with little or no overshoot and to maintain the control signal within the power supplies limitations. Chosen values for Q_{ds} and R_{ds} are

$$Q_{ds} = \begin{bmatrix} Q_{sp} & Q_{sv} & Q_{su} \end{bmatrix} \quad (9)$$
$$Q_{sp} = diag\begin{bmatrix} 5\times10^4 & 5\times10^4 & 5\times10^4 & 5\times10^4 & 4\times10^4 & 3\times10^4 \end{bmatrix}$$
$$Q_{sv} = 0_{6\times6}$$
$$Q_{su} = 10^{-3} I_{6\times6}$$
$$R_{ds} = I_{6\times6}$$

Here Q_{sp} is the matrix penalising angular positions, Q_{sv} is for the velocities and Q_{su} is for the integral

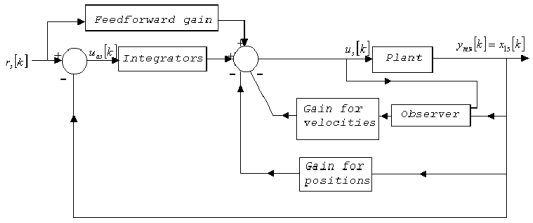

Fig. 3.1 Observer-based control system for the sagittal plane

actions. In selecting Q_{sp} it was desirable for them to be as low as possible to prevent demands for large control signals. Low Q_{sp} values increase relative stability and reduce sensitivity to noise. On the other hand, to track reference signals with small errors and quickly attenuate disturbances, relatively high values of Q_{sp} are needed. Therefore, a compromise was made between relative stability margins and tracking of reference signals. To reduce the magnitude of the control signals, the velocity penalty matrix, Q_{sv}, is set to zero. In the sagittal plane, gains for integral actions were kept to minimum. High integral gains tend to cause oscillations in the system, mainly due to the presence of backlash. The control system for the lateral plane has the same structure as the one for the sagittal plane. The only difference is that in the lateral plane there are four links instead of six. The matrices Q_{dl} and R_{dl} for the performance index are

$$Q_{dl} = \begin{bmatrix} Q_{lp} & Q_{lv} & Q_{lu} \end{bmatrix}$$
$$Q_{lp} = diag\begin{bmatrix} 5\times10^4 & 5\times10^4 & 5\times10^4 & 5\times10^4 \end{bmatrix}$$
$$Q_{lv} = 0_{4\times4}$$
$$Q_{lu} = diag\begin{bmatrix} 1\times10^{-3} & 1.2\times10^{-2} & 1\times10^{-1} & 1.2\times10^{-2} \end{bmatrix}$$
$$R_{dl} = I_{4\times4}$$

Due to high static friction of the worm gearboxes used for the lateral hip joints, the integral penalty matrix Q_{lu} is given higher values than those in the sagittal plane.

4. RELATIVE STABILITY AND PERFORMANCE

This section investigates the robustness of the control system through the analysis of Nyquist and singular value plots. The state space representation of the overall controller can be written as follows (sub-index *s* is used for the sagittal plane and *l* for the lateral plane):

$$\tilde{a}_s = \begin{bmatrix} F_s - H_s L12_s & -H_s L2_s \\ 0 & I_{6\times6} \end{bmatrix}$$
$$\tilde{b}_s = \begin{bmatrix} E_s - H_s\left(L11_s + L12_s K_s\right) \\ -I_{6\times6} \end{bmatrix}$$
$$\tilde{c}_s = -\begin{bmatrix} L12_s & L2_s \end{bmatrix}$$

$$\tilde{d}_s = -(L11_s + L12_s K_s)$$
$$\tilde{g}_s = \begin{bmatrix} H_s L11_s \\ I_{6\times 6} \end{bmatrix} \qquad (10)$$

Defining

$$G_{cs}(z) = \tilde{c}_s (zI - \tilde{a}_s)^{-1} \tilde{b}_s + \tilde{d}_s$$
$$N_s(z) = \tilde{c}_s (zI - \tilde{a}_s)^{-1} \tilde{g}_s + L11_s \qquad (11)$$
$$G_s(z) = C_s (zI - A_s)^{-1} B_s$$
$$G_s^{dist}(z) = C_s (zI - A_s)^{-1} B_s^{dist}$$

Then equations (2) and (5) can be written as

$$x_{s1}(z) = G_s(z)u(z) + G_s^{dist}\tau_s(z)$$
$$u_s(z) = G_{cs}(z)[x_{s1}(z) + n_s(z)] + N_s(z)r_s(z) \qquad (12)$$

Here, n_s represents quantization measurement noise. The corresponding block diagram is shown in Figure 4.1, where d_s represents contributions from torque disturbances. The pre-filter $P_s(z)$ can be used to limit angular velocities, to reduce large sudden demands in the control signals or to carry out smooth transitions between different reference set-points. The design of the control system does not include the effects of the smoothing filters (at 15 Hz) and the anti-aliasing filters (at 22 Hz). However, their effects on the robustness of the control system are investigated through Nyquist plots of the determinant of return difference matrices. The return difference equations at the plant input and output are given below for sagittal plane

$$F_{os}(z) = I - G_s(z)G_{cs}(z)$$
$$F_{is}(z) = I - G_{cs}(z)G_s(z) \qquad (13)$$

The control system shown in Figure 4.1 can be expressed as

$$y_{ms}(z) = S_{os}(z)d_s(z) + G_{ys}(z)y_{rs}(z) + T_{os}(z)n_s(z) \qquad (14)$$

$$u_s(z) = G_{us}(z)y_{rs}(z) + T_{is}(z)(d_s(z) + n_s(z)) \qquad (15)$$

$$S_{os}(z) = F_{os}(z)^{-1}$$
$$S_{is}(z) = F_{is}(z)^{-1}$$
$$G_{ys}(z) = S_{os}(z)G_s(z)N_s(z)P_s(z)$$
$$T_{os}(z) = S_{os}(z)G_s(z)G_{cs}(z)$$
$$G_{us}(z) = S_{is}(z)N_s(z)P_s(z)$$
$$T_{is}(z) = S_{is}(z)G_{cs}(z)$$

The above analysis can be carried out for the plant together with the smoothing and anti-aliasing filters, i.e. replace $G_s(z)$ by $G_{fs}(z)$ after appending all the relevant filters dynamics. For the equations in the lateral plane, the sub-index *s* is replaced by *l*.

Figure 4.2 shows the Nyquist plots of $\det(F_{os})$ and $\det(F_{ol})$ around the critical point (note that $\det(F_{os}) = \det(F_{is})$). For the sagittal plane, the origin is encircled four times in an anticlockwise direction. For the lateral plane, three encirclements of the origin occur. We point out that the number of encirclements is equal to the number of unstable open loop eigenvalues of each model (sagittal or lateral plane) provided that the controller (10) has no eigenvalues outside the unit circle. The Nyquist plots clearly indicate that the anti-aliasing and smoothing filters have reduced the relative stability of the control system.

Fig. 4.1 Control system block diagram (drawn for the sagittal plane)

Figures 4.3 - 4.6 show the singular value plots of the transfer matrices given by equations (14)-(15) with and without the filters. Again, the analysis with nominal design has better gain characteristics. Figure 4.3 shows the transmission from output disturbance to the plant output. In the sagittal plane, the plot shows that up to 0.8 Hz any output disturbances are attenuated by the control system. Above 0.8 Hz disturbances can be amplified, especially around 8 Hz. Also, the analysis with the filters shows degradation in performance. In the lateral plane, the system is susceptible to disturbances above 0.8 Hz. Figure 4.4 shows the transmission of reference signals at the plant output (cut-off frequencies about 1 Hz and 1.5 Hz). Both analyses are shown without pre-filters. Step reference signals can produce angular velocities in excess of 1rad/s. For such speeds, the linearized model will be less accurate than the non-linear model (1) due to terms involving squared angular velocities. Therefore, in the experimental evaluation we have used unity gain pre-filters (about 0.16 Hz bandwidth) to keep angular velocities smaller than 1rad/s. Noise transmission characteristics at the plant output are shown in Figure 4.5. In the sagittal plane, measurement noise begins to be attenuated above 8 Hz. In the lateral plane the performance is slightly better, noise attenuation occurs above 4 Hz. Sources of noise are due to quantization errors of about $\pm$ 0.5mrad. Contribution of disturbances and noise to the control effort are presented in Figure 4.6. The experimental data gathered from joint positions indicated that quantization is the main source for noise, and its amplitude is $\pm$ 0.5mrad. Maximum amplification in the sagittal plane is 56dB (Figure 4.6). This may produce a control effort around 0.31V. This voltage level is not large enough to drive any joints, since a voltage of around 0.5V is needed to overcome stiction. Therefore, the control efforts are not significantly contaminated by quantization noise.

5. CONCLUSIONS

In this paper, we have presented an approach for stabilisation of a 12 DOF biped robot using LQR theory and reduced order observers. The theoretical analysis indicates that the design technique is robust against disturbances or noise. The control systems were designed using single support models. Experimental tests have shown that the controllers worked well during both single and double support phases. The control system was capable of maintaining joint positions close to given reference values under small torque disturbances. For large torque disturbances the biped did not remain standing. This failure was due to the lack of information about ground reaction forces. It is clear that ground reaction force measurements are essential to maintain equilibrium in realistic situations.

REFERENCES

Amirouche, F. M. L., (1992), "*Computational methods in multibody dynamics*", Prentice-Hall, New Jersey.

Channon P. H., Hopkins S. H., and Pham D. T., (1992), "Modelling and control of a bipedal robot", *Journal of Systems Engineering*, **vol. 2**, pp 46-59.

Eldukhri, E. E., (1996), "Design and control of a biped walking robot", PhD Thesis, Dept. Electronic and Electrical Engineering, University of Salford, UK.

Hemami, H. and Wyman, B. F., (1979), "Modeling and control of constrained dynamic systems with application to biped locomotion in the frontal plane", *IEEE Trans. on Automatic Control*, **vol. AC-24**, no.4, pp 527-535.

Hirai, K., Hirose, M., Haikawa, Y. and Takenaka, T., (1998), " The development of Honda humanoid robot", *IEEE International Conference on Robotics and Automation*, **vol. 2**, Leuven, Belgium, May 1998, pp 1321-1326.

Golliday, C. L. Jr. and Hemami, H., (1976), "Postural stability of the two-degree of freedom biped by general linear feedback", *IEEE Trans. on Automatic Control*, **vol. AC-21**, no.1, pp 74-79.

Golliday, C. L. Jr. and Hemami, H., (1977), "An approach to analyzing biped locomotion dynamics and designing robot locomotion controls", *IEEE Trans. on Automatic Control*, **vol. AC-22**, no.6, pp 963-972.

Inaba, M., Kanehiro, F., Kagami, S., and Inoue, H., (1995), "Two-armed Bipedal Robot that can Walk, Roll Over and Stand up", *IROS'95 International Conference on Intelligent Robots and System*, **vol. 3**, Pittsburgh, Pennsylvania, U. S.A., pp 297-302.

Lewis, F.L., Abdallah, C.T. and Dawson, D.M., (1993), "*Control of Robot Manipulators*", Mcmillan Publishing Company, New York.

Li, Q., Takanishi, A. and Kato, I., (1993), "Learning control for a biped walking robot with a trunk", *IEEE Int. Conference on Intelligent Robots and Systems*, Yokohama, Japan, July 1993, pp 1171-1777.

Medrano-Cerda, G. A. and Eldukhri, E. E., (1997), "Biped robot locomotion in the sagittal plane", *Trans. Inst. Measurement and Control*, **vol. 19**, No: 1, pp 38-49.

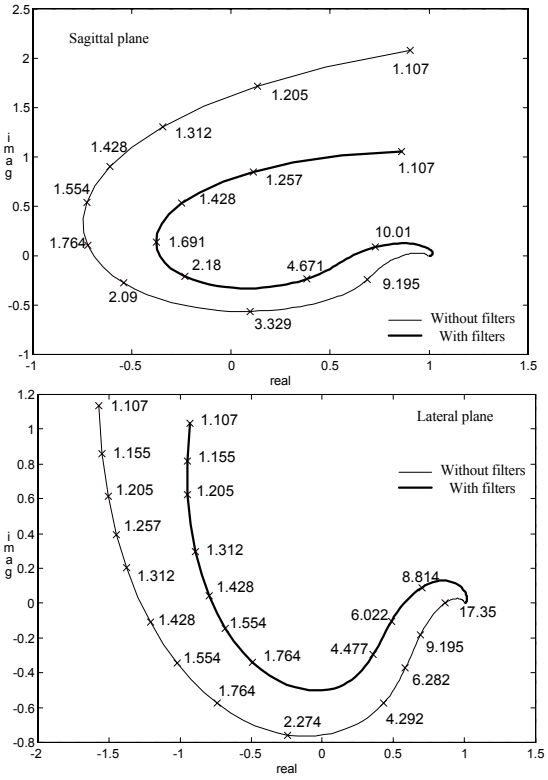

Fig. 4.2 Nyquist plots of $\det(F_{os})$ and $\det(F_{ol})$

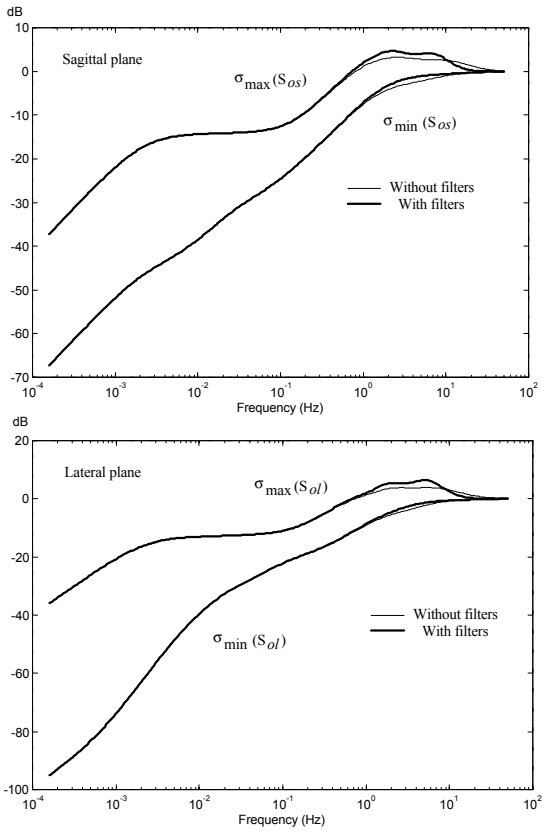

Fig. 4.3 Singular value plots of the sensitivity matrices $S_{os}(z)$, $S_{ofs}(z)$, $S_{ol}(z)$ and $S_{ofl}(z)$

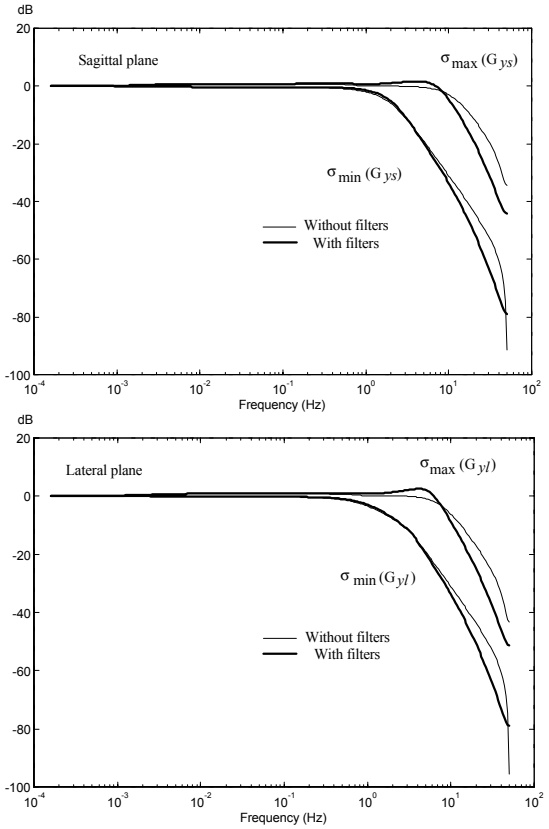

Fig. 4.4 Singular value plots of the transfer matrices $G_{ys}(z)$, $G_{yfs}(z)$, $G_{yl}(z)$ and $G_{yfl}(z)$

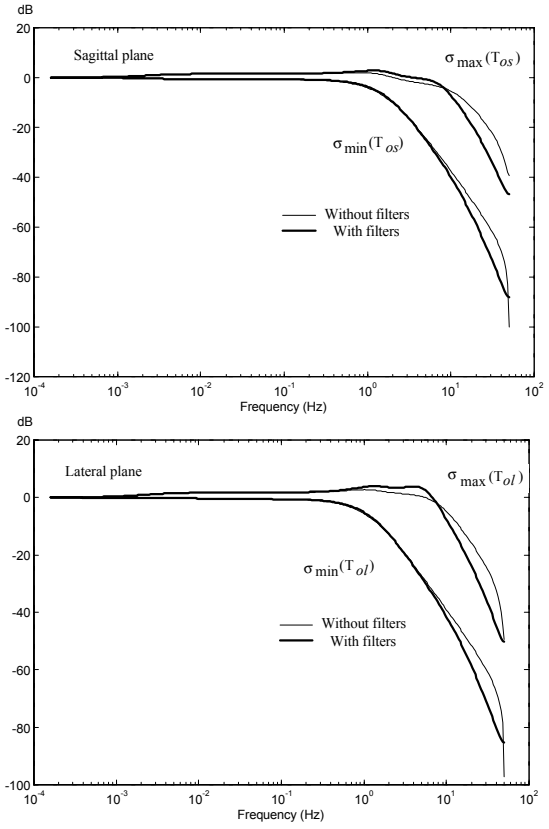

Fig. 4.5 Singular value plots of the complementary sensitivity matrices $T_{os}(z)$, $T_{ofs}(z), T_{ol}(z)$ and $T_{ofl}(z)$

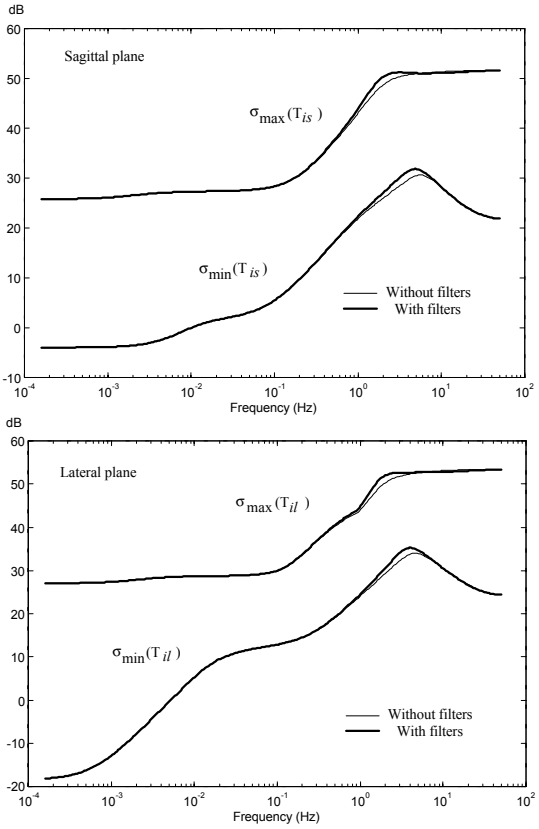

Fig. 4.6 Singular value plots of transfer matrices $T_{is}(z)$, $T_{ifs}(z)$, $T_{il}(z)$ and $T_{ifl}(z)$

Mita, T., Yamaguchi, T., Kashiwase, T., and Kawase T., (1984), "'Realization of a High Speed Biped Using Modern Control Theory", *Int. J. Control*, **vol. 40**, No. 1, pp 107-119.

Miura, H., Shimoyama, I., (1984), "Dynamic Walk of a Robot", *Int. J. Robotics Research*, **vol. 3**, no. 2, pp 60-74.

Raibert, M. H., (1986), *"Legged Robots That Balance*", Cambridge, Mass., MIT Press.

Takanishi, A., Ishida, M., Yamazaki, Y. and Kato, I., (1985), "The Realization of dynamic walking by the biped walking robot WL-10RD", *Int. Conference on Advanced Robotics*, Tokyo, pp 459-466.

Takanishi, A., Tochizawa, M., Takeya, T., Kanaki, H. and Kato, I., (1990), "Realization of dynamic biped walking stabilized with trunk motion under known external force", *4th Int. Conference on Advanced Robotics*, Columbus, Ohio. Also, in *Scientific Fundamentals of Robotics 7*, Waldron, K.J., Editor, Springer-Verlag, Berlin, pp 299-310.

Vukobratovic, M., Borovac, B., Surla, D. and Stokic, D., (1990), "*Biped Locomotion: Dynamics, Stability, Control and Application*", Springer-Verlag, Berlin.

Yamaguchi, J., Soga, E., Inoue, S., and Takanishi, A., (1999), "Development of a bipedal humanoid robot: Control method of whole body co-operative dynamic biped walking", *IEEE International Conference on Robotics and Automation*, Detroit, Michigan, May 1999, pp 368-374.